Article

Changes in Surface Hydrophobicity of Coal Particles and the Formation of Coarse Particle–Bubble Clusters in the Process of High-Intensity Conditioning

Xiaofu Jia, Yuexian Yu *[ID]**, Jiahui Liu, Chen Min, Fan Liu, Ningning Zhang, Songjiang Chen and Zhanglei Zhu**

College of Chemistry and Chemical Engineering, Xi'an University of Science and Technology, Xi'an 710054, China; jamie202212@163.com (X.J.)

* Correspondence: yuyuexian2011@163.com

Abstract: The mechanism of high-intensity conditioning (HIC) has not been thoroughly revealed, and therefore this work investigates the effect of HIC on the surface hydrophobicity of coal with different particle sizes and the possible formation of particle–bubble clusters. The results show that different HIC conditions are required for coarse and fine particles. Coarse particles (+75 μm) require a higher turbulence intensity to increase collector dispersion, thereby increasing the adsorption of the collector. Fine particles (−75 μm) require a lower turbulence intensity to reduce the desorption of the collector. In this study, the optimum HIC conditions for coarse and fine particles are "2200 rpm + 1 min" and "1300 rpm + 1 min", respectively. Interestingly, it seems that the adsorption capacity between fine particles and the collector is weaker than that for coarse particles. A non-enclosed HIC system produces up to 1.78×10^4/g bubbles in coarse particle–bubble clusters, and the mean bubble diameter is approximately 87 μm. The cluster achieves pre-mineralization and increases the apparent particle size, which is expected to improve flotation.

Keywords: coal flotation; high-intensity conditioning; particle surface hydrophobicity; particle–bubble cluster

1. Introduction

Flotation uses the difference in surface properties between valuable minerals and gangue minerals to selectively separate them and is often used to separate fine minerals [1–4]. Pulp conditioning is usually required prior to flotation [5]. Pulp conditioning is an important part of the flotation process and is beneficial in improving the yield of cleaned coal and combustible matter recovery. High-intensity conditioning (HIC) can not only make the pulp reach a suitable and stable concentration, but can also destroy the fine particle floc, reduce the slime coating, modify the surface, disperse the flotation reagents, promote effective contact between the reagents and coal particles, and create a good mineralization condition for subsequent flotation operations. Currently, the essence of pulp conditioning is creating a strong turbulent movement of liquid flow through strong mechanical agitation, and finding the suitable conditioning strength and time is the key to improve the particles' hydrophobicity. HIC has been widely used in the industry, and many new types of pulp conditioning equipment have been developed and applied in practice. Traditional mechanical stirring conditioning technology continues to develop and enrich [6].

The influence of HIC on the flotation effect has been extensively studied before, and the surface modification of coal particles, reagent dispersion, and effective collision between the reagents and coal particles constitute the main mechanisms of HIC [7]. Wang et al. [8] studied the effect of shearing intensity on dispersion characteristics and flotation recovery of coal by using a mechanical flotation cell. It was found that flotation recovery was positively correlated with shear intensity. Zhao et al. [9] found that increasing the shear

rate was beneficial to the flocculation of hydrophobic particles. Yu et al. [10] found that the hydrophilic high-ash slime on the surface of coal particles is removed after HIC, and the adsorption of collectors with coal particles and the flotation recovery both significantly increased. Chen et al. [11] found that HIC could remove the hydrophilic gangue slime from coarse pentlandite particle surfaces, with the amount removed depending upon both the intensity and duration of agitation. During the HIC process, impeller blades create turbulence for bubble-particle interaction and cause increased turbulence which makes fine slime detach from coarse particles [12,13]. Additionally, high speed turbulence can generate small bubbles, increase bubble-particle collision, and improving fine particle recovery [14,15]. It is noteworthy that the more intense the turbulence, the better the effect of HIC. However, due to the effect of bypass and resolution probability, over-conditioning is detrimental to improving the recovery of clean coal. A suitable HIC environment can fully disperse the pulp and reagents, increase the probability of collision between the regents and the particles [7,16–18], and contribute significantly to coal flotation.

It was also observed that particle aggregates are favorable to particle–bubble interaction. Particle–bubble interaction relates to particle hydrophobicity and the bubbles generated on the solid particle surface, and these changes have an additional effect on the surface hydrophobicity of coal [19,20]. Furthermore, in the process of HIC, the air can be sucked into the pulp and shredded into small bubbles by the turbulence [12,13]. Additionally, these small bubbles potentially precipitate on the coal surface due to the hydrophobic interaction, thereby forming particle–bubble clusters. This cluster is expected to improve flotation [21–23]. Ata et al., [21] investigated the characteristics of clusters formed in the flotation of silica and found that most of the bubbles appear to be in the form of clusters held together with bridging particles. Zhang et al., [22,23] found that the attachment of one or more additional bubbles will increase its buoyancy above the level necessary to raise it in the flotation cell. Thus, the cluster formation is able to increase the flotation recovery of coarse particles. The upper size range of particles that can be recovered in conventional machines could be extended by the use of bubble clusters. In addition, the cluster increases the apparent area of the particles. Therefore, the particles are more likely to collide with reagent droplets, improving the flotation.

However, the mechanism of fluid shear on mineral particle surface hydrophobicity improvement is still unclear and needs to be further explored from more aspects. There is a lack of research on changes in the surface hydrophobicity of coarse and fine coal particles in the process of HIC. Due to the complexity of factors affecting HIC, as well as the limitations in research methods and detection techniques, the mechanism of HIC has not been fully revealed. This study aims to investigate the effect of HIC on the surface hydrophobicity of coal particles with different sizes, and on the formation of particle–bubble clusters, providing a theoretical reference for further understanding the mechanism of HIC and optimizing the HIC process.

2. Materials and Methods

2.1. Samples and Experimental Devices

The coal sample used in the experiment was the flotation feed of a coking-coal preparation plant in Shanxi province, China. The particle size and ash distribution of the raw coal samples are shown in Table 1. It can be seen that the particle size of the coal sample is generally fine, and the yield of the −0.045 mm fraction is 60.90%, which is beyond the range of easy-to-float coal particle sizes. The −0.075 mm fraction contains a large number of impurities with a 38.04% ash content, posing great threats to the flotation due to the potential water entrainment and slime coatings [24]. The total ash content of the flotation feed is up to 30.16%, and it is speculated that this coal sample is difficult to float.

Table 1. Analyses of particle size and ash content of raw coal samples.

Particle Size/mm	Yield/%	Ash/%	Positive Cumulative		Negative Cumulative	
			Yield/%	Ash/%	Yield/%	Ash/%
+0.5	0.40	5.72	0.40	5.72	100.00	30.16
0.5–0.25	4.85	5.89	5.25	5.88	99.60	30.26
0.25–0.125	14.33	11.44	19.58	9.95	94.75	31.50
0.125–0.075	12.69	19.28	32.28	13.62	80.42	35.08
0.075–0.045	6.82	26.71	39.10	15.90	67.72	38.04
−0.045	60.90	39.31	100.00	30.16	60.90	39.31
Total	100.00	30.16				

Both the measurement of coarse particle–bubble clusters and the HIC tests were conducted in a self-made stirring device. The structure of the stirring device is shown in Figure 1. The stirring device consists of a stirring tank and four pitched blades, driven by a benchtop drilling machine (ZHX-13, China West-lake), which could provide a speed range of 515 rpm~1580 rpm. The four pitched blades were kept in the same position in the stirring tank for each experiment, and the stirring tank was equipped with a lid. The HIC environment was non-enclosed since the tank was connected to the outside air through a small hole in the lid. For each HIC test, 80 g of coal sample was added to the conditioning tank with 800 mL of tap water and 72 μL of diesel. Stirring tests were performed at various conditioning speeds and conditioning times.
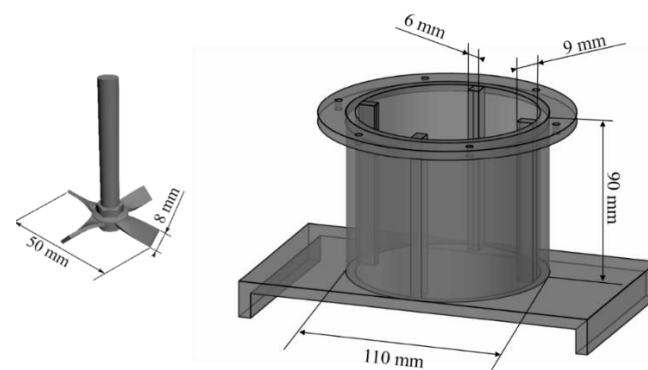
Figure 1. Structure diagram of the stirring device.

2.2. Single Bubble Loading Area and Contact Angle Measurements

Single bubble loading capacity and contact angle measurements were carried out on the coal samples which were treated by HIC to comprehensively analyze the changes in coal particle hydrophobicity after HIC [25]. The effects of different HIC conditions on single bubble loading capacity and contact angle were investigated. The concentration of the pulp is 100 g/L during HIC, and the dosage of diesel was 0.7515 kg/t. After HIC, the pulp was wet-sieved using a 75 μm-mesh sieve, and the product above the sieve and under the sieve was dried at 32 °C and set aside. Only the fraction of +75 μm was subjected to the single bubble loading capacity test because the −75 μm fraction failed to reach the single bubble loading capacity test due to its cloudy suspension. Both the sieving products were subjected to contact angle measurements.

The illustration of bubble loading capacity measurement is shown in Figure 2. For each measurement, 0.6 g of coal was taken and placed into a 5 cm high cube glass vessel followed by 60 mL of tap water. The cube glass vessel was stirred by a magnetic stirrer at a constant speed of 200 rpm. A bubble of about 2 mm in diameter was produced each time by an autosampler and was fixed at 2 cm below the water surface centrally. The images of bubble loading were recorded at 15 s, 30 s, 45 s, and 60 s. After taking the bubble loading photos, the bubble loading area was calculated by using ImageJ software as shown in

Figure 2. By setting the known diameter (fixed at 2 mm for each test) of the bubble as the standard meter scale of the image, the value of the bubble loading area can be automatically calculated by manually selecting the outside edge of the particles loaded on the bubble surface [26,27]. The area marked in the red circle is the defined area of the bubble load. All tests were repeated three times and the results were averaged.
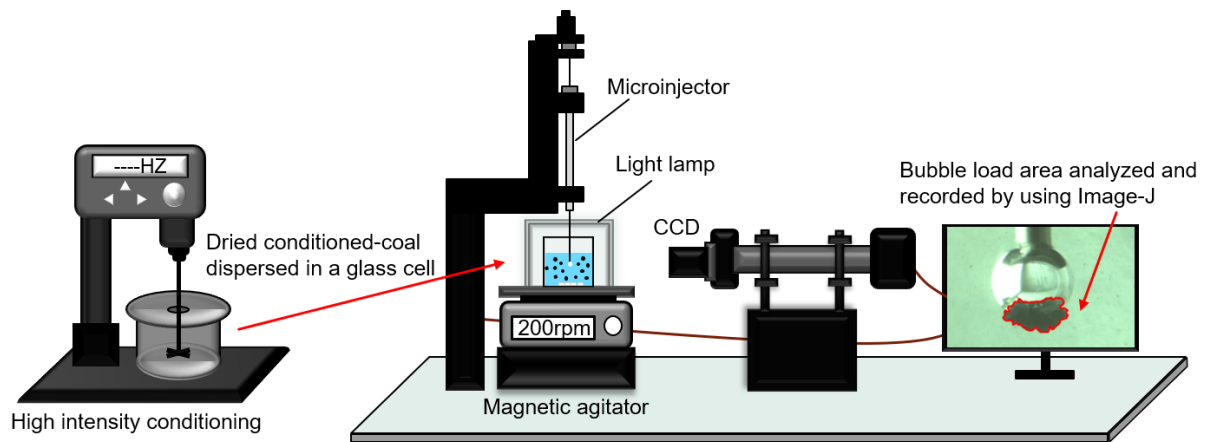

Figure 2. Illustration of the bubble loading capacity measurement.

The contact angle was measured using the sessile drop method (CA-100B, Shanghai, China, Yingnuo). Each time, about 1 g of coal powders were pelletized directly into a tablet with a diameter of about 15 mm and a thickness of about 2 mm, without grinding to avoid the potential destruction of surface hydrophobicity. The contact angle was measured twice at different positions on the same tablet and the results were averaged. Since the coal powders were not ground further, the change of contact angle directly reflected the changes in the surface hydrophobicity of the coal particles.

2.3. Measurement of Coarse Particle–Bubble Clusters

For the test of the formation of the coarse particle–bubble cluster, to establish a clear observation scene for the optical microscope the samples were first purified by flotation before the tests to eliminate fine fractions of high-ash slime. Thus, the +75 μm fraction of flotation clean coal was used as the final test sample. The clustering behavior of the coarse particles (+75 μm) and bubbles under different conditioning parameters was investigated using an optical microscope (Leica DM4500P, Wetzlar, Germany). For each test, about 0.3 mL of a stirred pulp (0.6% (*w/w*)) suspension of coal particles was carefully dropped onto a glass slide, and a coverslip was placed over the droplet to expel the air between the two slides so that the pulp was fully spread between the slides. The microscope lens magnification used was fixed at 320× and the microscopic images were transmitted to a computer via a CCD camera as shown in Figure 3. The number of bubbles contained in the whole droplet was counted, and the number of bubbles attached to the unit mass of coal was obtained by dividing the number of bubbles by the weight of the dry coal contained in the droplet. The bubble diameters were measured using the system software Measure Kit. To reveal the source of the bubbles in the clusters, the changes in the stirring device when the water was stirred alone were observed and analyzed using a high-speed dynamic camera (OLYMPUS i-SPEED 3, Tokyo, Japan).
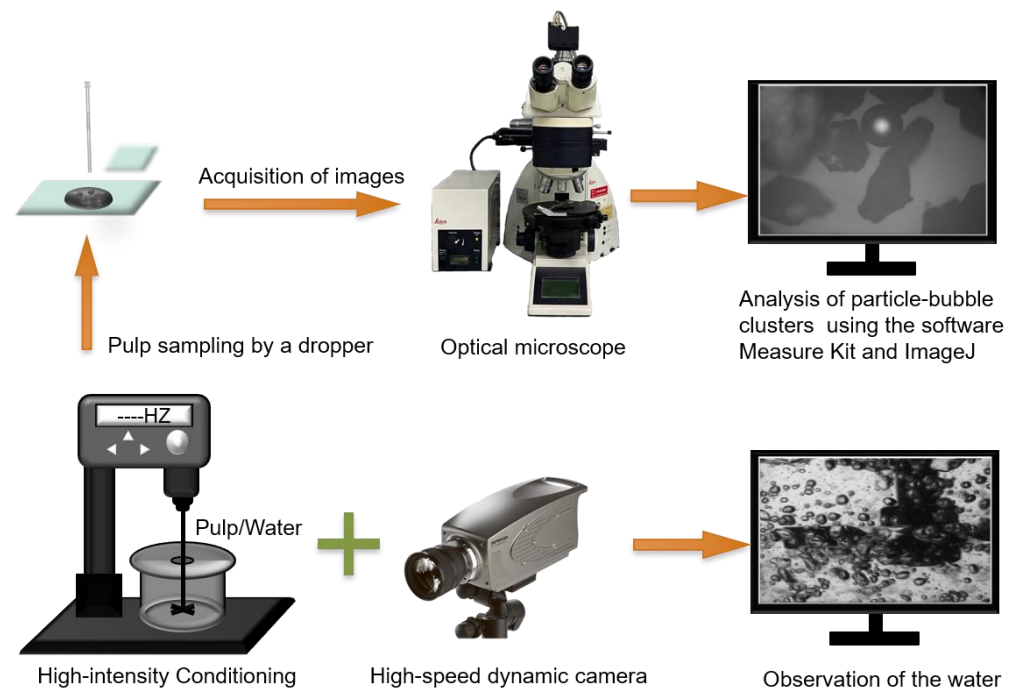
Figure 3. Illustration of observation of coarse particle–bubble clusters and water.

3. Results and Discussion

3.1. Results of Single Bubble Loading Capacity

The bubble loading capacity is able to sensitively detect changes in the surface hydrophobicity of coal particles. The larger the area of the bubble load, the better the surface hydrophobicity of the particles [28,29]. The bubble loading areas corresponding to different conditioning speeds are shown in Figure 4a. It can be seen that the bubble loading area increases gradually with the increasing interaction time at each conditioning speed. At the 60th second, the difference between the bubble loading areas achieved at each conditioning speed (except 1300 rpm) was not significant, 1.38 mm^2, 1.22 mm^2, 1.26 mm^2, and 1.34 mm^2, respectively, and it is assumed that almost the same ultimate bubble loading area will be achieved at each conditioning speed with the further extension of the interaction time. The smallest bubble loading area was obtained at the speed of 1300 rpm, which shows that a low conditioning speed is less effective than a high conditioning speed in improving the hydrophobicity of coal particles. After 60 s of interaction, the growth rates of the bubble loading area for each conditioning speed were 60.66%, 55.35%, 46.23%, 65.11%, and 57.45%, respectively (the growth rates of the bubble loading area are calculated as $(A_{60s} - A_{15s})/A_{60s}$, A refers to bubble loading area). It can be seen that the bubble loading area growth rate corresponding to 2200 rpm is the largest, which indicates the best effect on improving the surface hydrophobicity of coal. Compared to 2200 rpm, the bubble loading area growth rate decreased by 7.66 percentage points when the conditioning speed increased to 2500 rpm due to the fluid bypass and the effects of reagent desorption [7,16]. It is evident that an insufficient or excessive conditioning speed fails to improve the surface hydrophobicity of coal particles [30]. Therefore, there is an optimal conditioning speed for HIC.

As shown in Figure 4b, when the conditioning time was 1 min the bubble loading area increased sharply in the first 30 s of interaction time and then increased slowly to 1.26 mm^2 when the interaction time reached the 60th second, with a growth rate of 65.11%. After conditioning for 2 min, the bubble loading area gradually increased to 1.13 mm^2 with the extension of the interaction time, and the growth rate was 59.97%. When the conditioning time was 3 min, the bubble loading area increased rapidly and then leveled off after the 30th second and finally reached 1.04 mm^2 at the 60th second, with a growth

rate of 45.87%. Obviously, the bubble loading area and bubble-loading-area-growth rate were highest after 1-min conditioning, and too long a conditioning time was not conducive to the hydrophobicity improvement of coal particles. This is probably because an excessive conditioning time causes reagent desorption from the coal surface and re-adsorption of high-ash slime onto the coal surface, resulting in a decrease in the hydrophobicity of the coal particles [7,31].
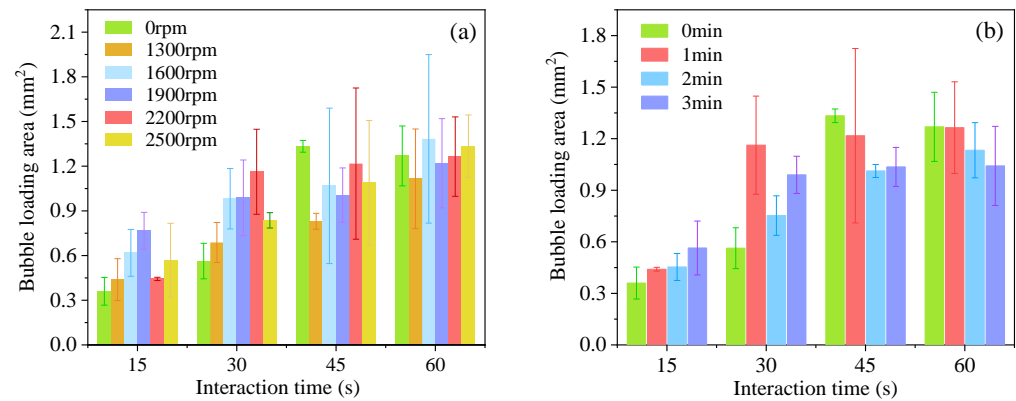

Figure 4. Bubble loading area of +75 μm fraction at different HIC conditions, (**a**) conditioning speed, (**b**) conditioning time.

To sum up, for the coal sample (+75 μm) in this test the optimal HIC condition was "2200 rpm + 1 min", below or above which the surface hydrophobicity of the coal particles decreases.

3.2. Results of Contact Angle Measurement

From Figure 5a,b, it can be seen that the maximum contact angle of +75 μm fraction was obtained with 1-min conditioning at 2200 rpm, which is consistent with the conclusion drawn from the bubble loading test shown in Figure 4. This indicates that, for coarse particles, the increase in the conditioning speed within a certain range facilitates the increase in the contact angle. With the increase in conditioning speed, the number of effective collisions between particles and reagents increases, and the higher conditioning speed provides greater momentum for the collisions between oil droplets and particles, so that the oil droplets overcome the electrostatic repulsion and cross the energy barrier. However, the adsorbed oil droplets desorbed from the particle surface as the conditioning speed increased to 2500 rpm [32]. The situation for fine coal particles, however, is different. As shown in Figure 5a, the contact angle of fine coal particles decreases sharply to 48.53° as the conditioning speed increases within the range of 1300 rpm to 1900 rpm. Therefore, this indirectly shows that the collector adsorbed on the surface of fine particles gradually decreases with increasing conditioning speed. This indicates that, within the speed range of 1300 rpm to 1900 rpm, the coarse and fine particles are in competition for adsorption with the collector. And the adsorption capacity between fine particles and the collector is weaker than that for coarse particles. Interestingly, this is contrary to the conventional understanding that fine particles have priority in the adsorption of reagents due to their larger specific surface area.
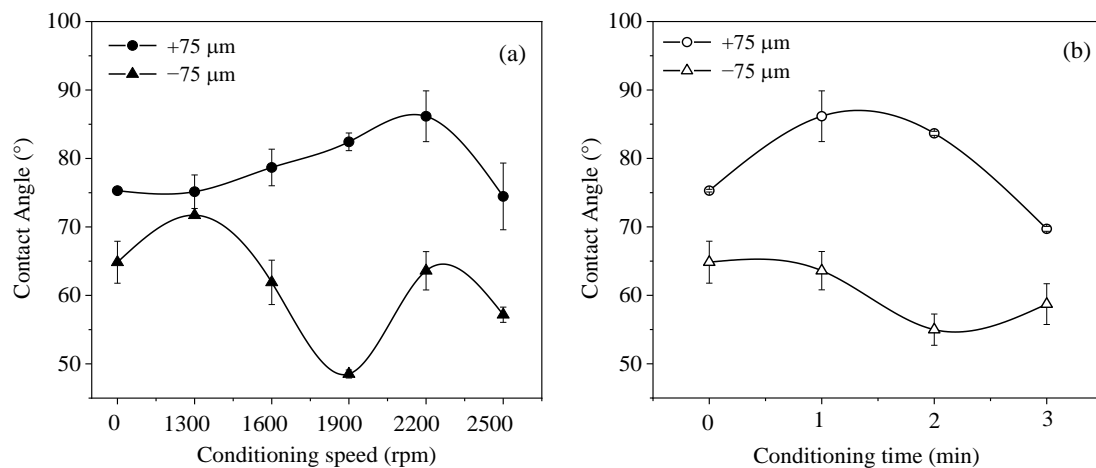
Figure 5. The contact angle of coarse and fine particles at different HIC conditions, (**a**) conditioning speed, (**b**) conditioning time.

From Figure 5, it can be concluded that different HIC conditions are required for coarse and fine particles. Coarse particles (+75 μm) require higher turbulence intensity to improve collector dispersion and adsorption. However, fine particles (−75 μm) require a lower turbulence intensity to reduce the desorption of the collector. Blindly increasing turbulence intensity to improve the hydrophobicity of fine particles is futile; a better approach is to maintain low turbulence intensity while improving reagent dispersion. The improvement effect of HIC on fine particle flotation is mainly due to shear flocculation, which is sensitive to turbulence intensity. Previous research shows that significant shear flocculation can be achieved at a relatively low turbulence intensity [33]. Therefore, it is possible to treat collector dispersion as an independent unit (such as collector online ultrasonic emulsification operation); in this way, it is beneficial to find a lower turbulence intensity that can simultaneously meet the needs of coarse and fine particles, which is conducive to achieve a low-energy consumption but high-efficiency HIC process.

3.3. Results of Coarse Particle–Bubble Cluster Measurement

The changes in the stirring device, when the water was stirred alone by the four pitched blades, were observed using a high-speed dynamic camera as shown in Figure 6. It was confirmed that in the non-enclosed HIC system, shear stirring can produce a large number of bubbles in the water. As is shown in Figure 6, a higher speed is more likely to produce smaller bubbles. It can also be seen that as the stirring speed increases, the turbulence intensity of the fluid increases under the impeller's propulsion, and a vortex is generated at the location of the central axis of stirring. It is known from Bernoulli's law that the greater the velocity of the fluid, the smaller the pressure, so the air above the vortex is continuously sucked into the liquid due to the differential pressure thus forming bubbles [34,35]. Bubbles in the turbulent flow are further shredded into smaller bubbles, as shown in Figure 6c. Therefore, the air sucked into the pulp is one of the important sources of bubbles in the coarse particle–bubble clusters.
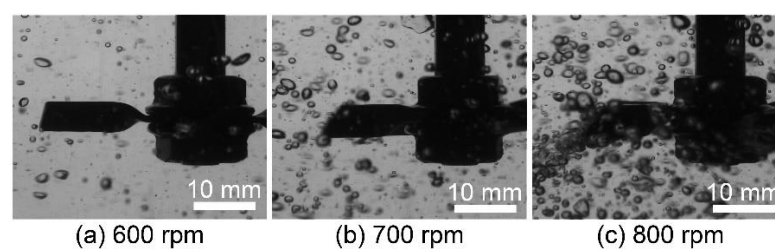

Figure 6. Changes in the stirring device when water is stirred alone at different stirring speeds, (**a**) 600 rpm, (**b**) 700 rpm, (**c**) 800 rpm.

From Figure 7a, it can be seen that the number of bubbles in the cluster increased continuously, but the diameter of the bubble decreased with the increase in the conditioning speed. At the conditioning speed of 2500 rpm, the number of bubbles contained per gram of coal reached 1.78×10^4, while the mean bubble diameter decreased to a minimum value of 87 μm. This is consistent with the conclusion drawn in Figure 6 that the amount of air sucked in the pulp increases as the conditioning speed increases and large bubbles are crushed into smaller bubbles. Therefore, the number of bubbles keeps increasing but the diameter of the bubbles gradually decreases.
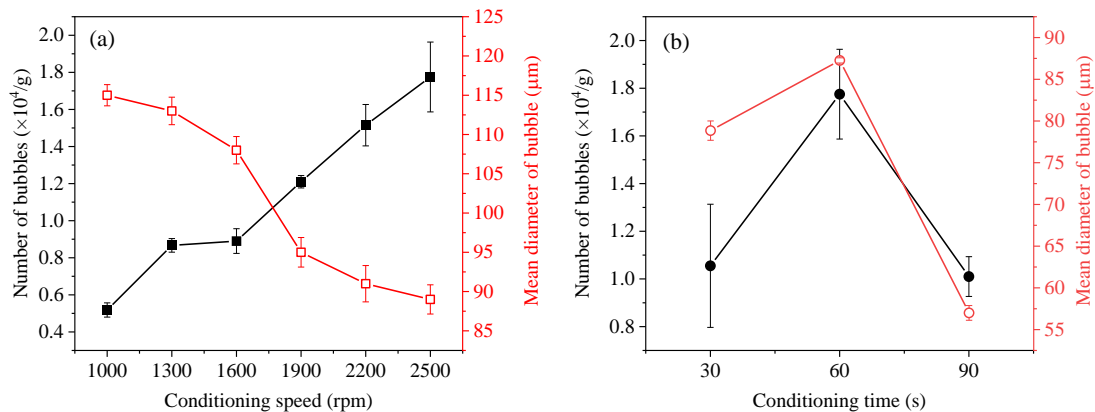

Figure 7. Effect of conditioning speed and time on the number and diameter of bubbles in coarse particle–bubble clusters (+75 μm coal), (**a**) effect of the conditioning speed, (**b**) effect of the conditioning time.

From Figure 7b, it can be seen that the number of bubbles increases and then decreases with the increase in conditioning time. During HIC, the bubbles continuously collide and adhere to the particles in turbulent flow, which is beneficial to the adsorption of bubbles to particles. However, the centrifugal force caused by the eddy also leads to the desorption of particles from bubbles. Therefore, desorption and adsorption occur simultaneously. Figure 7b shows that an excessive conditioning time leads to a decrease in the number of bubbles in the clusters, and that the optimal conditioning time is 60 s. The smaller the diameter of the bubble, the stronger the adhesion force between it and the particles, making it less likely to desorb. Therefore, the mean diameter of the bubbles in the clusters decreases from 87 μm to 57 μm when the conditioning time increases to 90 s as shown in Figure 7b. From another perspective, the bubble size in the clusters can be regulated by controlling the conditioning time.

It can be seen from Figure 8 that the bubbles and coal particles bridge each other to form particle–bubble clusters and to realize pre-mineralization. At the same time, the discrete particles are agglomerated into larger particle–bubble clusters, increasing the apparent size of the particles, which is beneficial to the subsequent flotation [36,37]. It was observed that the bubbles in the clusters can exist stably for several hours. In addition, under the high-intensity conditioning speed of 2500 rpm, there are still a large number of particle–bubble clusters. These clusters can even rise to the gas–liquid interface by means of their own buoyancy. In addition, it was observed that the minimum diameter of the bubbles can reach ~10 μm, but such tiny and stable bubbles only account for a very small number of bubbles, and the diameter of most bubbles is between 50 and 120 μm. It is certain that particle–bubble clusters will have a positive effect on flotation, which is consistent with the findings of Sun et al. [38,39].
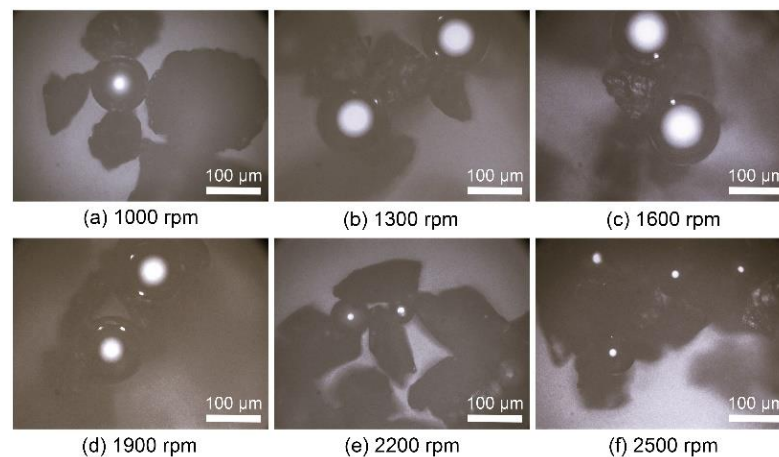
Figure 8. Micrographs of coarse coal-bubble clusters at different conditioning speeds (1 min of conditioning time).

4. Conclusions

In this paper, changes in the surface hydrophobicity of coarse and fine coal particles after HIC were studied. At the same time, the behavior of coarse particle–bubble clusters under fluid shearing was studied using an optical microscope and a high-speed dynamic camera. The main conclusions arrived at are as follows:

(1) There is an optimal conditioning speed and time for +75 μm coal. In this work, the optimal HIC conditions are "2200 rpm + 1 min". Below or above this threshold, the surface hydrophobicity of coal particles decreases.

(2) In this research, within the speed range of 1300 rpm to 1900 rpm, the coarse and fine particles are in competition for adsorption with the collector. Interestingly, the adsorption capacity between fine particles and the collector is weaker than that for coarse particles.

(3) The non-enclosed HIC system can promote the formation of coarse particle-bubble clusters. Particle-bubble clusters produce pre-mineralization and increase the apparent size of particles, which is expected to benefit the flotation of coal. The number of bubbles in the cluster is as high as 1.78×10^4/g, and the smallest mean bubble diameter is about 87 μm.

(4) The operating conditions of HIC required for coarse and fine particles are different. For coarse particles, a higher turbulence intensity is required to increase collector dispersion, and thereby facilitating the adsorption between particles and collectors. However, for fine particles, a relatively lower turbulence intensity is required to reduce the desorption of the collector from the particle's surface.

Author Contributions: X.J.: Investigation, Data curation, Writing—Original draft preparation. Y.Y.: Conceptualization, Methodology, Writing—Reviewing and Editing, Supervision. J.L.: Investigation. C.M.: Data curation. F.L.: Investigation. N.Z.: Validation. S.C.: Validation. Z.Z.: Validation. All authors have read and agreed to the published version of the manuscript.

Institutional Review Board Statement: Not applicable.

Informed Consent Statement: Not applicable.

Data Availability Statement: Not applicable.

Conflicts of Interest: The authors declare no conflict of interest.

References

1. Oats, W.J.; Ozdemir, O.; Nguyen, A.V. Effect of mechanical and chemical clay removals by hydrocyclone and dispersants on coal flotation. *Miner. Eng.* **2010**, *23*, 413–419. [CrossRef]
2. Melo, F.; Laskowski, J.S. Fundamental properties of flotation frothers and their effect on flotation. *Miner. Eng.* **2006**, *19*, 766–773. [CrossRef]
3. Cheng, G.; Li, Y.; Cao, Y.; Zhang, Z. A novel method for the desulfurization of medium–high sulfur coking coal. *Fuel* **2023**, *335*, 126988. [CrossRef]
4. Cheng, G.; Zhang, M.; Zhang, Y.; Lin, B.; Zhan, H.; Zhang, H. A novel renewable collector from waste fried oil and its application in coal combustion residuals decarbonization. *Fuel* **2022**, *323*, 124388. [CrossRef]
5. Engel, M.D.; Middlebrook, P.D.; Jameson, G.J. Advances in the study of high intensity conditioning as a means of improving mineral flotation performance. *Miner. Eng.* **1997**, *10*, 55–68. [CrossRef]
6. Li, Y.; Zhang, X.; Gui, X. The morphological feature of hard-to-float fine coal and enhancing its floatability by stirring. *J. China Univ. Min. Technol.* **2012**, *41*, 930–935.
7. Ma, L.; Wei, L.; Li, J.; Chen, Q. Theoretical study and application of efficient coal slurry conditioning. *J. China Univ. Min. Technol.* **2012**, *41*, 315–320.
8. Wang, H.; Zhu, H.; Zhu, J.; Shao, S.; Huang, D.; Liu, J.; Li, T. Effect of energy consumption on dispersion and recovery of coal slimes in a mechanical flotation cell. *Energy Sources Part A Recovery Util. Environ. Eff.* **2020**, *42*, 1882–1890. [CrossRef]
9. Zhao, J.; Hu, Y.; Liu, J.; Wang, J. Hydrophobic Flocculation of Coal Particles Controlled by Mechanical Stirring. *Miner. Process. Extr. Metall. Rev.* **2022**, 1–6. [CrossRef]
10. Yu, Y.; Ma, L.; Wu, L.; Ye, G.; Sun, X. The role of surface cleaning in high intensity conditioning. *Powder Technol.* **2017**, *319*, 26–33. [CrossRef]
11. Chen, G.; Grano, S.; Sobieraj, S.; Ralston, J. The effect of high intensity conditioning on the flotation of a nickel ore. Part 1: Size-by-size analysis. *Miner. Eng.* **1999**, *12*, 1185–1200. [CrossRef]
12. Gorain, B.K.; Franzidis, J.P.; Manlapig, E.V. Flotation Cell Design: Application of Fundamental Principles. *Encycl. Sep. Sci.* **2000**, *143*, 1502–1512.
13. Wills, B.A.; Finch, J. *Wills' Mineral Processing Technology: An Introduction to the Practical Aspects of Ore Treatment and Mineral Recovery*, 8th ed.; Elsevier Science and Technology Books, Inc.: Amsterdam, The Netherlands, 2016; p. 512.
14. Farrokhpay, S.; Filippov, L.; Fornasiero, D. Flotation of Fine Particles: A Review. *Min. Proc. Ext. Met. Rev.* **2021**, *42*, 473–483. [CrossRef]
15. Wang, D.W.; Liu, Q. Hydrodynamics of froth flotation and its effects on fine and ultrafine mineral particle flotation: A literature review. *Miner. Eng.* **2021**, *173*, 107220. [CrossRef]
16. Ma, L.; Wei, L.; Jiang, X.; Zhao, X.; Chen, Q. Effects of shearing strength in slurry conditioning on coal slime flotation. *J. China Coal Soc.* **2013**, *38*, 140–144.
17. Koh, P.; Schwarz, M.P. CFD model of a self-aerating flotation cell. *Int. J. Miner. Process.* **2007**, *85*, 16–24. [CrossRef]
18. Gomez-Flores, A.; Heyes, G.W.; Ilyas, S.; Kim, H. Effects of artificial impeller blade wear on bubble–particle interactions using CFD (k–ε and LES), PIV, and 3D printing. *Miner. Eng.* **2022**, *186*, 107766. [CrossRef]
19. Hampton, M.A.; Nguyen, A.V. Accumulation of dissolved gases at hydrophobic surfaces in water and sodium chloride solutions: Implications for coal flotation. *Miner. Eng.* **2009**, *22*, 786–792. [CrossRef]
20. Seddon, J.R.T.; Lohse, D.; Ducker, W.A.; Craig, V.S.J. A deliberation on nanobubbles at surfaces and in bulk. *ChemPhysChem* **2012**, *13*, 2179–2187. [CrossRef] [PubMed]
21. Ata, S.; Jameson, G.J. The formation of bubble clusters in flotation cells. *Int. J. Miner. Process.* **2005**, *76*, 123–139. [CrossRef]
22. Chen, Z.; Ata, S.; Jameson, G.J. Behaviour of bubble clusters in a turbulent flotation cell. *Powder Technol.* **2015**, *269*, 337–344. [CrossRef]
23. Chen, Z.; Ata, S.; Jameson, G.J. Breakup and re-formation of bubble clusters in a flotation cell. *Miner. Eng.* **2015**, *71*, 16–20. [CrossRef]
24. Chen, X.; Peng, Y. Managing clay minerals in froth flotation—A critical review. *Miner. Process. Extr. Metall. Rev.* **2018**, *39*, 289–307. [CrossRef]
25. Wang, A.; Geoffrey, E.; Subhasish, M. A review of bubble surface loading and its effect on bubble dynamics. *Miner. Eng.* **2023**, *199*, 108105. [CrossRef]
26. Xia, W.; Ma, G.; Bu, X.; Peng, Y. Effect of particle shape on bubble-particle attachment angle and flotation behavior of glass beads and fragments. *Powder Technol.* **2018**, *338*, 168–172. [CrossRef]
27. Wang, P.; Cilliers, J.J.; Neethling, S.J.; Brito-Parada, P.R. The behavior of rising bubbles covered by particles. *Chem. Eng. J.* **2019**, *365*, 111–120. [CrossRef]
28. Liang, L.; Li, Q.; Hu, P.; Xie, G. Influence law of slime coating on coal floatability. *J. China Coal Soc.* **2021**, *46*, 2793–2803.
29. Zhang, H.; Wang, H.; Chen, R.; Yan, X.; Zheng, K.; Li, D.; Jiang, S. Turbulence enhancement mechanism of coal slime pulp conditioning and new type vortex enhancing pulp conditioning process. *J. China Coal Soc.* **2022**, *47*, 934–944.
30. Yoon, R.H.; Luttrell, G.H. The Effect of Bubble Size on Fine Particle Flotation. *Miner. Process. Extr. Metall. Rev.* **1989**, *5*, 101–122. [CrossRef]

31. Burat, F.; Sirkeci, A.A.; Onal, G. Improved Fine Coal Dewatering by Ultrasonic Pretreatment and Dewatering Aids. *Miner. Process. Extr. Metall. Rev.* **2015**, *36*, 129–135. [CrossRef]

32. Song, S.; Lopez-Valdivieso, A. Parametric aspect of hydrophobic flocculation technology. *Miner. Process. Extr. Metall. Rev.* **2002**, *23*, 101–127. [CrossRef]

33. Bu, X.; Danstan, J.K.; Hassanzadeh, A.; Vakylabad, A.B.; Chelgani, S.C. Metal extraction from ores and waste materials by ultrasound-assisted leaching—An overview. *Miner. Process. Extr. Metall. Rev.* **2022**, *volume*, 1–18. [CrossRef]

34. Huang, J.; Sun, L.; Du, M.; Liang, Z.; Mo, Z.; Tang, J.; Xie, G. An investigation on the performance of a micro-scale Venturi bubble generator. *Chem. Eng. J.* **2020**, *386*, 120980. [CrossRef]

35. Zhao, L.; Sun, L.; Mo, Z.; Du, M.; Huang, J.; Bao, J.; Tang, J.; Xie, G. Effects of the divergent angle on bubble transportation in a rectangular Venturi channel and its performance in producing fine bubbles. *Int. J. Multiph. Flow* **2019**, *114*, 192–206. [CrossRef]

36. Tao, D.; Yu, S.; Zhou, X.; Honaker, R.Q.; Parekh, B.K. Picobubble column flotation of fine coal. *Int. J. Coal Prep. Util.* **2008**, *28*, 1–14. [CrossRef]

37. Zhou, W.; Chen, H.; Ou, L.; Shi, Q. Aggregation of ultra-fine scheelite particles induced by hydrodynamic cavitation. *Int. J. Miner. Process.* **2016**, *157*, 236–240. [CrossRef]

38. Sun, Y.; Xie, G.; Peng, Y.; Chen, Y.; Ma, G. How does high intensity conditioning affect flotation performance? *Int. J. Coal Prep. Util.* **2019**, *39*, 302–316. [CrossRef]

39. Yu, Y.; Liu, J.; Jia, X.; Min, C.; Liu, F.; Zhang, N.; Chen, S.; Zhu, Z.; Zhou, A. A new perspective on the understanding of high-intensity conditioning: Incompatibility of conditions required for coarse and fine coal particles. *Miner. Process. Extr. Metall. Rev.* **2022**, 1–10. [CrossRef]